PHYSICAL REVIEW D **71,** 051502(R) (2005)

Measurement of the $\overline{B}^0 \to D^{*+}\ell^-\overline{\nu}_\ell$ decay rate and $|V_{cb}|$

B. Aubert,[1] R. Barate,[1] D. Boutigny,[1] F. Couderc,[1] J.-M. Gaillard,[1] A. Hicheur,[1] Y. Karyotakis,[1] J. P. Lees,[1] V. Tisserand,[1] A. Zghiche,[1] A. Palano,[2] A. Pompili,[2] J. C. Chen,[3] N. D. Qi,[3] G. Rong,[3] P. Wang,[3] Y. S. Zhu,[3] G. Eigen,[4] I. Ofte,[4] B. Stugu,[4] G. S. Abrams,[5] A. W. Borgland,[5] A. B. Breon,[5] D. N. Brown,[5] J. Button-Shafer,[5] R. N. Cahn,[5] E. Charles,[5] C. T. Day,[5] M. S. Gill,[5] A. V. Gritsan,[5] Y. Groysman,[5] R. G. Jacobsen,[5] R. W. Kadel,[5] J. Kadyk,[5] L. T. Kerth,[5] Yu. G. Kolomensky,[5] G. Kukartsev,[5] G. Lynch,[5] L. M. Mir,[5] P. J. Oddone,[5] T. J. Orimoto,[5] M. Pripstein,[5] N. A. Roe,[5] M. T. Ronan,[5] V. G. Shelkov,[5] W. A. Wenzel,[5] M. Barrett,[6] K. E. Ford,[6] T. J. Harrison,[6] A. J. Hart,[6] C. M. Hawkes,[6] S. E. Morgan,[6] A. T. Watson,[6] M. Fritsch,[7] K. Goetzen,[7] T. Held,[7] H. Koch,[7] B. Lewandowski,[7] M. Pelizaeus,[7] M. Steinke,[7] J. T. Boyd,[8] N. Chevalier,[8] W. N. Cottingham,[8] M. P. Kelly,[8] T. E. Latham,[8] F. F. Wilson,[8] T. Cuhadar-Donszelmann,[9] C. Hearty,[9] N. S. Knecht,[9] T. S. Mattison,[9] J. A. McKenna,[9] D. Thiessen,[9] A. Khan,[10] P. Kyberd,[10] L. Teodorescu,[10] V. E. Blinov,[11] V. P. Druzhinin,[11] V. B. Golubev,[11] V. N. Ivanchenko,[11] E. A. Kravchenko,[11] A. P. Onuchin,[11] S. I. Serednyakov,[11] Yu. I. Skovpen,[11] E. P. Solodov,[11] A. N. Yushkov,[11] D. Best,[12] M. Bruinsma,[12] M. Chao,[12] I. Eschrich,[12] D. Kirkby,[12] A. J. Lankford,[12] M. Mandelkern,[12] R. K. Mommsen,[12] W. Roethel,[12] D. P. Stoker,[12] C. Buchanan,[13] B. L. Hartfiel,[13] S. D. Foulkes,[14] J. W. Gary,[14] B. C. Shen,[14] K. Wang,[14] D. del Re,[15] H. K. Hadavand,[15] E. J. Hill,[15] D. B. MacFarlane,[15] H. P. Paar,[15] Sh. Rahatlou,[15] V. Sharma,[15] J. W. Berryhill,[16] C. Campagnari,[16] B. Dahmes,[16] S. L. Levy,[16] O. Long,[16] A. Lu,[16] M. A. Mazur,[16] J. D. Richman,[16] W. Verkerke,[16] T. W. Beck,[17] A. M. Eisner,[17] C. A. Heusch,[17] W. S. Lockman,[17] T. Schalk,[17] R. E. Schmitz,[17] B. A. Schumm,[17] A. Seiden,[17] P. Spradlin,[17] D. C. Williams,[17] M. G. Wilson,[17] J. Albert,[18] E. Chen,[18] G. P. Dubois-Felsmann,[18] A. Dvoretskii,[18] D. G. Hitlin,[18] I. Narsky,[18] T. Piatenko,[18] F. C. Porter,[18] A. Ryd,[18] A. Samuel,[18] S. Yang,[18] S. Jayatilleke,[19] G. Mancinelli,[19] B. T. Meadows,[19] M. D. Sokoloff,[19] T. Abe,[20] F. Blanc,[20] P. Bloom,[20] S. Chen,[20] W. T. Ford,[20] U. Nauenberg,[20] A. Olivas,[20] P. Rankin,[20] J. G. Smith,[20] J. Zhang,[20] L. Zhang,[20] A. Chen,[21] J. L. Harton,[21] A. Soffer,[21] W. H. Toki,[21] R. J. Wilson,[21] Q. L. Zeng,[21] D. Altenburg,[22] T. Brandt,[22] J. Brose,[22] M. Dickopp,[22] E. Feltresi,[22] A. Hauke,[22] H. M. Lacker,[22] R. Müller-Pfefferkorn,[22] R. Nogowski,[22] S. Otto,[22] A. Petzold,[22] J. Schubert,[22] K. R. Schubert,[22] R. Schwierz,[22] B. Spaan,[22] J. E. Sundermann,[22] D. Bernard,[23] G. R. Bonneaud,[23] F. Brochard,[23] P. Grenier,[23] S. Schrenk,[23] Ch. Thiebaux,[23] G. Vasileiadis,[23] M. Verderi,[23] D. J. Bard,[24] P. J. Clark,[24] D. Lavin,[24] F. Muheim,[24] S. Playfer,[24] Y. Xie,[24] M. Andreotti,[25] V. Azzolini,[25] D. Bettoni,[25] C. Bozzi,[25] R. Calabrese,[25] G. Cibinetto,[25] E. Luppi,[25] M. Negrini,[25] L. Piemontese,[25] A. Sarti,[25] E. Treadwell,[26] R. Baldini-Ferroli,[27] A. Calcaterra,[27] R. de Sangro,[27] G. Finocchiaro,[27] P. Patteri,[27] M. Piccolo,[27] A. Zallo,[27] A. Buzzo,[28] R. Capra,[28] R. Contri,[28] G. Crosetti,[28] M. Lo Vetere,[28] M. Macri,[28] M. R. Monge,[28] S. Passaggio,[28] C. Patrignani,[28] E. Robutti,[28] A. Santroni,[28] S. Tosi,[28] S. Bailey,[29] G. Brandenburg,[29] M. Morii,[29] E. Won,[29] R. S. Dubitzky,[30] U. Langenegger,[30] W. Bhimji,[31] D. A. Bowerman,[31] P. D. Dauncey,[31] U. Egede,[31] J. R. Gaillard,[31] G. W. Morton,[31] J. A. Nash,[31] G. P. Taylor,[31] M. J. Charles,[32] G. J. Grenier,[32] U. Mallik,[32] J. Cochran,[33] H. B. Crawley,[33] J. Lamsa,[33] W. T. Meyer,[33] S. Prell,[33] E. I. Rosenberg,[33] J. Yi,[33] M. Davier,[34] G. Grosdidier,[34] A. Höcker,[34] S. Laplace,[34] F. Le Diberder,[34] V. Lepeltier,[34] A. M. Lutz,[34] T. C. Petersen,[34] S. Plaszczynski,[34] M. H. Schune,[34] L. Tantot,[34] G. Wormser,[34] C. H. Cheng,[35] D. J. Lange,[35] M. C. Simani,[35] D. M. Wright,[35] A. J. Bevan,[36] C. A. Chavez,[36] J. P. Coleman,[36] I. J. Forster,[36] J. R. Fry,[36] E. Gabathuler,[36] R. Gamet,[36] R. J. Parry,[36] D. J. Payne,[36] R. J. Sloane,[36] C. Touramanis,[36] J. J. Back,[37] C. M. Cormack,[37] P. F. Harrison,[37,*] F. Di Lodovico,[37] G. B. Mohanty,[37] C. L. Brown,[38] G. Cowan,[38] R. L. Flack,[38] H. U. Flaecher,[38] M. G. Green,[38] P. S. Jackson,[38] T. R. McMahon,[38] S. Ricciardi,[38] F. Salvatore,[38] M. A. Winter,[38] D. Brown,[39] C. L. Davis,[39] J. Allison,[40] N. R. Barlow,[40] R. J. Barlow,[40] P. A. Hart,[40] M. C. Hodgkinson,[40] G. D. Lafferty,[40] A. J. Lyon,[40] J. C. Williams,[40] A. Farbin,[41] W. D. Hulsbergen,[41] A. Jawahery,[41] D. Kovalskyi,[41] C. K. Lae,[41] V. Lillard,[41] D. A. Roberts,[41] G. Blaylock,[42] C. Dallapiccola,[42] K. T. Flood,[42] S. S. Hertzbach,[42] R. Kofler,[42] V. B. Koptchev,[42] T. B. Moore,[42] S. Saremi,[42] H. Staengle,[42] S. Willocq,[42] R. Cowan,[43] G. Sciolla,[43] F. Taylor,[43] R. K. Yamamoto,[43] D. J. J. Mangeol,[44] P. M. Patel,[44] S. H. Robertson,[44] A. Lazzaro,[45] F. Palombo,[45] J. M. Bauer,[46] L. Cremaldi,[46] V. Eschenburg,[46] R. Godang,[46] R. Kroeger,[46] J. Reidy,[46] D. A. Sanders,[46] D. J. Summers,[46] H. W. Zhao,[46] S. Brunet,[47] D. Côté,[47] P. Taras,[47] H. Nicholson,[48] N. Cavallo,[49] F. Fabozzi,[49,†] C. Gatto,[49] L. Lista,[49] D. Monorchio,[49] P. Paolucci,[49] D. Piccolo,[49] C. Sciacca,[49] M. Baak,[50] H. Bulten,[50] G. Raven,[50] L. Wilden,[50] C. P. Jessop,[51] J. M. LoSecco,[51] T. A. Gabriel,[52] T. Allmendinger,[53] B. Brau,[53] K. K. Gan,[53] K. Honscheid,[53] D. Hufnagel,[53] H. Kagan,[53] R. Kass,[53] T. Pulliam,[53] A. M. Rahimi,[53] R. Ter-Antonyan,[53] Q. K. Wong,[53] J. Brau,[54] R. Frey,[54] O. Igonkina,[54] C. T. Potter,[54] N. B. Sinev,[54] D. Strom,[54] E. Torrence,[54] F. Colecchia,[55] A. Dorigo,[55] F. Galeazzi,[55] M. Margoni,[55] M. Morandin,[55] M. Posocco,[55] M. Rotondo,[55] F. Simonetto,[55] R. Stroili,[55] G. Tiozzo,[55] C. Voci,[55] M. Benayoun,[56] H. Briand,[56] J. Chauveau,[56] P. David,[56] Ch. de la Vaissière,[56] L. Del Buono,[56] O. Hamon,[56] M. J. J. John,[56] Ph. Leruste,[56] J. Malcles,[56] J. Ocariz,[56] M. Pivk,[56] L. Roos,[56] S. T'Jampens,[56] G. Therin,[56]

P. F. Manfredi,[57] V. Re,[57] P. K. Behera,[58] L. Gladney,[58] Q. H. Guo,[58] J. Panetta,[58] F. Anulli,[27,59] M. Biasini,[59] I. M. Peruzzi,[27,59] M. Pioppi,[59] C. Angelini,[60] G. Batignani,[60] S. Bettarini,[60] M. Bondioli,[60] F. Bucci,[60] G. Calderini,[60] M. Carpinelli,[60] V. Del Gamba,[60] F. Forti,[60] M. A. Giorgi,[60] A. Lusiani,[60] G. Marchiori,[60] F. Martinez-Vidal,[60,‡] M. Morganti,[60] N. Neri,[60] E. Paoloni,[60] M. Rama,[60] G. Rizzo,[60] F. Sandrelli,[60] J. Walsh,[60] M. Haire,[61] D. Judd,[61] K. Paick,[61] D. E. Wagoner,[61] N. Danielson,[62] P. Elmer,[62] Y. P. Lau,[62] C. Lu,[62] V. Miftakov,[62] J. Olsen,[62] A. J. S. Smith,[62] A. V. Telnov,[62] F. Bellini,[63] G. Cavoto,[62,63] R. Faccini,[63] F. Ferrarotto,[63] F. Ferroni,[63] M. Gaspero,[63] L. Li Gioi,[63] M. A. Mazzoni,[63] S. Morganti,[63] M. Pierini,[63] G. Piredda,[63] F. Safai Tehrani,[63] C. Voena,[63] S. Christ,[64] G. Wagner,[64] R. Waldi,[64] T. Adye,[65] N. De Groot,[65] B. Franek,[65] N. I. Geddes,[65] G. P. Gopal,[65] E. O. Olaiya,[65] R. Aleksan,[66] S. Emery,[66] A. Gaidot,[66] S. F. Ganzhur,[66] P.-F. Giraud,[66] G. Hamel de Monchenault,[66] W. Kozanecki,[66] M. Langer,[66] M. Legendre,[66] G. W. London,[66] B. Mayer,[66] G. Schott,[66] G. Vasseur,[66] Ch. Yèche,[66] M. Zito,[66] M. V. Purohit,[67] A. W. Weidemann,[67] J. R. Wilson,[67] F. X. Yumiceva,[67] D. Aston,[68] R. Bartoldus,[68] N. Berger,[68] A. M. Boyarski,[68] O. L. Buchmueller,[68] M. R. Convery,[68] M. Cristinziani,[68] G. De Nardo,[68] D. Dong,[68] J. Dorfan,[68] D. Dujmic,[68] W. Dunwoodie,[68] E. E. Elsen,[68] S. Fan,[68] R. C. Field,[68] T. Glanzman,[68] S. J. Gowdy,[68] T. Hadig,[68] V. Halyo,[68] C. Hast,[68] T. Hryn'ova,[68] W. R. Innes,[68] M. H. Kelsey,[68] P. Kim,[68] M. L. Kocian,[68] D. W. G. S. Leith,[68] J. Libby,[68] S. Luitz,[68] V. Luth,[68] H. L. Lynch,[68] H. Marsiske,[68] R. Messner,[68] D. R. Muller,[68] C. P. O'Grady,[68] V. E. Ozcan,[68] A. Perazzo,[68] M. Perl,[68] S. Petrak,[68] B. N. Ratcliff,[68] A. Roodman,[68] A. A. Salnikov,[68] R. H. Schindler,[68] J. Schwiening,[68] G. Simi,[68] A. Snyder,[68] A. Soha,[68] J. Stelzer,[68] D. Su,[68] M. K. Sullivan,[68] J. Va'vra,[68] S. R. Wagner,[68] M. Weaver,[68] A. J. R. Weinstein,[68] W. J. Wisniewski,[68] M. Wittgen,[68] D. H. Wright,[68] A. K. Yarritu,[68] C. C. Young,[68] P. R. Burchat,[69] A. J. Edwards,[69] T. I. Meyer,[69] B. A. Petersen,[69] C. Roat,[69] S. Ahmed,[70] M. S. Alam,[70] J. A. Ernst,[70] M. A. Saeed,[70] M. Saleem,[70] F. R. Wappler,[70] W. Bugg,[71] M. Krishnamurthy,[71] S. M. Spanier,[71] R. Eckmann,[72] H. Kim,[72] J. L. Ritchie,[72] A. Satpathy,[72] R. F. Schwitters,[72] J. M. Izen,[73] I. Kitayama,[73] X. C. Lou,[73] S. Ye,[73] F. Bianchi,[74] M. Bona,[74] F. Gallo,[74] D. Gamba,[74] M. Bomben,[75] C. Borean,[75] L. Bosisio,[75] C. Cartaro,[75] F. Cossutti,[75] G. Della Ricca,[75] S. Dittongo,[75] S. Grancagnolo,[75] L. Lanceri,[75] P. Poropat,[75,§] L. Vitale,[75] G. Vuagnin,[75] R. S. Panvini,[76] Sw. Banerjee,[77] C. M. Brown,[77] D. Fortin,[77] P. D. Jackson,[77] R. Kowalewski,[77] J. M. Roney,[77] H. R. Band,[78] S. Dasu,[78] M. Datta,[78] A. M. Eichenbaum,[78] M. Graham,[78] J. J. Hollar,[78] J. R. Johnson,[78] P. E. Kutter,[78] H. Li,[78] R. Liu,[78] A. Mihalyi,[78] A. K. Mohapatra,[78] Y. Pan,[78] R. Prepost,[78] A. E. Rubin,[78] S. J. Sekula,[78] P. Tan,[78] J. H. von Wimmersperg-Toeller,[78] J. Wu,[78] S. L. Wu,[78] Z. Yu,[78] M. G. Greene,[79] and H. Neal[79]

(*BABAR* Collaboration)

[1]*Laboratoire de Physique des Particules, F-74941 Annecy-le-Vieux, France*
[2]*Università di Bari, Dipartimento di Fisica and INFN, I-70126 Bari, Italy*
[3]*Institute of High Energy Physics, Beijing 100039, China*
[4]*University of Bergen, Institute of Physics, N-5007 Bergen, Norway*
[5]*Lawrence Berkeley National Laboratory and University of California, Berkeley, California 94720, USA*
[6]*University of Birmingham, Birmingham, B15 2TT, United Kingdom*
[7]*Ruhr Universität Bochum, Institut für Experimentalphysik 1, D-44780 Bochum, Germany*
[8]*University of Bristol, Bristol BS8 1TL, United Kingdom*
[9]*University of British Columbia, Vancouver, British Columbia, Canada V6T 1Z1*
[10]*Brunel University, Uxbridge, Middlesex UB8 3PH, United Kingdom*
[11]*Budker Institute of Nuclear Physics, Novosibirsk 630090, Russia*
[12]*University of California at Irvine, Irvine, California 92697, USA*
[13]*University of California at Los Angeles, Los Angeles, California 90024, USA*
[14]*University of California at Riverside, Riverside, California 92521, USA*
[15]*University of California at San Diego, La Jolla, California 92093, USA*
[16]*University of California at Santa Barbara, Santa Barbara, California 93106, USA*
[17]*University of California at Santa Cruz, Institute for Particle Physics, Santa Cruz, California 95064, USA*
[18]*California Institute of Technology, Pasadena, California 91125, USA*
[19]*University of Cincinnati, Cincinnati, Ohio 45221, USA*
[20]*University of Colorado, Boulder, Colorado 80309, USA*
[21]*Colorado State University, Fort Collins, Colorado 80523, USA*
[22]*Technische Universität Dresden, Institut für Kern- und Teilchenphysik, D-01062 Dresden, Germany*
[23]*Ecole Polytechnique, LLR, F-91128 Palaiseau, France*
[24]*University of Edinburgh, Edinburgh EH9 3JZ, United Kingdom*
[25]*Università di Ferrara, Dipartimento di Fisica and INFN, I-44100 Ferrara, Italy*

[26]*Florida A&M University, Tallahassee, Florida 32307, USA*
[27]*Laboratori Nazionali di Frascati dell'INFN, I-00044 Frascati, Italy*
[28]*Università di Genova, Dipartimento di Fisica and INFN, I-16146 Genova, Italy*
[29]*Harvard University, Cambridge, Massachusetts 02138, USA*
[30]*Universität Heidelberg, Physikalisches Institut, Philosophenweg 12, D-69120 Heidelberg, Germany*
[31]*Imperial College London, London, SW7 2AZ, United Kingdom*
[32]*University of Iowa, Iowa City, Iowa 52242, USA*
[33]*Iowa State University, Ames, Iowa 50011-3160, USA*
[34]*Laboratoire de l'Accélérateur Linéaire, F-91898 Orsay, France*
[35]*Lawrence Livermore National Laboratory, Livermore, California 94550, USA*
[36]*University of Liverpool, Liverpool L69 72E, United Kingdom*
[37]*Queen Mary, University of London, E1 4NS, United Kingdom*
[38]*University of London, Royal Holloway and Bedford New College, Egham, Surrey TW20 0EX, United Kingdom*
[39]*University of Louisville, Louisville, Kentucky 40292, USA*
[40]*University of Manchester, Manchester M13 9PL, United Kingdom*
[41]*University of Maryland, College Park, Maryland 20742, USA*
[42]*University of Massachusetts, Amherst, Massachusetts 01003, USA*
[43]*Massachusetts Institute of Technology, Laboratory for Nuclear Science, Cambridge, Massachusetts 02139, USA*
[44]*McGill University, Montréal, Quebec, Canada H3A 2T8*
[45]*Università di Milano, Dipartimento di Fisica and INFN, I-20133 Milano, Italy*
[46]*University of Mississippi, University, Mississippi 38677, USA*
[47]*Université de Montréal, Laboratoire René J. A. Lévesque, Montréal, Quebec, Canada H3C 3J7*
[48]*Mount Holyoke College, South Hadley, Massachusetts 01075, USA*
[49]*Università di Napoli Federico II, Dipartimento di Scienze Fisiche and INFN, I-80126, Napoli, Italy*
[50]*NIKHEF, National Institute for Nuclear Physics and High Energy Physics, NL-1009 DB Amsterdam, The Netherlands*
[51]*University of Notre Dame, Notre Dame, Indiana 46556, USA*
[52]*Oak Ridge National Laboratory, Oak Ridge, Tennessee 37831, USA*
[53]*Ohio State University, Columbus, Ohio 43210, USA*
[54]*University of Oregon, Eugene, Oregon 97403, USA*
[55]*Università di Padova, Dipartimento di Fisica and INFN, I-35131 Padova, Italy*
[56]*Universités Paris VI et VII, Laboratoire de Physique Nucléaire et de Hautes Energies, F-75252 Paris, France*
[57]*Università di Pavia, Dipartimento di Elettronica and INFN, I-27100 Pavia, Italy*
[58]*University of Pennsylvania, Philadelphia, Pennsylvania 19104, USA*
[59]*Università di Perugia, Dipartimento di Fisica and INFN, I-06100 Perugia, Italy*
[60]*Università di Pisa, Dipartimento di Fisica, Scuola Normale Superiore and INFN, I-56127 Pisa, Italy*
[61]*Prairie View A&M University, Prairie View, Texas 77446, USA*
[62]*Princeton University, Princeton, New Jersey 08544, USA*
[63]*Università di Roma La Sapienza, Dipartimento di Fisica and INFN, I-00185 Roma, Italy*
[64]*Universität Rostock, D-18051 Rostock, Germany*
[65]*Rutherford Appleton Laboratory, Chilton, Didcot, Oxon, OX11 0QX, United Kingdom*
[66]*DSM/Dapnia, CEA/Saclay, F-91191 Gif-sur-Yvette, France*
[67]*University of South Carolina, Columbia, South Carolina 29208, USA*
[68]*Stanford Linear Accelerator Center, Stanford, California 94309, USA*
[69]*Stanford University, Stanford, California 94305-4060, USA*
[70]*State University of New York, Albany, New York 12222, USA*
[71]*University of Tennessee, Knoxville, Tennessee 37996, USA*
[72]*University of Texas at Austin, Austin, Texas 78712, USA*
[73]*University of Texas at Dallas, Richardson, Texas 75083, USA*
[74]*Università di Torino, Dipartimento di Fisica Sperimentale and INFN, I-10125 Torino, Italy*
[75]*Università di Trieste, Dipartimento di Fisica and INFN, I-34127 Trieste, Italy*
[76]*Vanderbilt University, Nashville, Tennessee 37235, USA*
[77]*University of Victoria, Victoria, British Columbia, Canada V8W 3P6*
[78]*University of Wisconsin, Madison, Wisconsin 53706, USA*
[79]*Yale University, New Haven, Connecticut 06511, USA*
(Received 11 August 2004; published 15 March 2005)

*Now at Department of Physics, University of Warwick, Coventry, United Kingdom.
†Also with Università della Basilicata, Potenza, Italy.
‡Also with IFIC, Instituto de Física Corpuscular, CSIC-Universidad de Valencia, Valencia, Spain.
§Deceased.

We present a measurement of the Cabibbo-Kobayashi-Maskawa matrix element $|V_{cb}|$ based on a sample of about 53 700 $\overline{B}^0 \to D^{*+}\ell^-\bar{\nu}_\ell$ decays observed by the *BABAR* detector. We obtain the branching fraction averaged over $\ell = e, \mu$, $\mathcal{B}(\overline{B}^0 \to D^{*+}\ell^-\bar{\nu}_\ell) = (4.90 \pm 0.07(\text{stat.})^{+0.36}_{-0.35}(\text{syst.}))\%$. We measure the differential decay rate as a function of w, the relativistic boost γ of the D^{*+} in the $\overline{B}^0$ rest frame. By extrapolating $d\Gamma/dw$ to the kinematic limit $w \to 1$, we extract the product of $|V_{cb}|$ and the axial form factor $\mathcal{A}_1(w = 1)$. We combine this measurement with a lattice QCD calculation of $\mathcal{A}_1(w = 1)$ to determine $|V_{cb}| = (38.7 \pm 0.3(\text{stat.}) \pm 1.7(\text{syst.})^{+1.5}_{-1.3}(\text{theory})) \times 10^{-3}$.

DOI: 10.1103/PhysRevD.71.051502 PACS numbers: 13.20.He, 11.30.Er, 12.15.Hh

In the standard model of electroweak interactions, the Cabibbo-Kobayashi-Maskawa (CKM) matrix describes the flavor mixing among quarks and determines the strength of CP violation by a single nontrivial weak phase. The CKM matrix element V_{cb} measures the weak coupling of the b to the c quark. In this Letter, we present measurements of the branching fraction $\mathcal{B}(\overline{B}^0 \to D^{*+}\ell^-\overline{\nu}_\ell)$ [1] and $|V_{cb}|$. The rate for this weak decay is proportional to $|V_{cb}|^2$ and is influenced by strong interactions through form factors, which are not known *a priori*. In the limit of infinite b-quark and c-quark masses, these form factors are determined by a single Isgur-Wise function [2]. The value of this function when the D^{*+} is at rest relative to the $\overline{B}^0$ has been computed for finite c- and b-quark masses using lattice QCD [3].

In this analysis, we measure the differential decay rate $d\Gamma/dw$, where w is the product of the four-velocities of the $\overline{B}^0$ and D^{*+}, and corresponds to the relativistic boost γ of the D^{*+} in the $\overline{B}^0$ rest frame. We extrapolate the rate to the zero-recoil limit $w = 1$, and use the theoretical result for the form factor there [3] to extract $|V_{cb}|$.

The analysis is based on a data sample of 79 fb^{-1} recorded on the $\Upsilon(4S)$ resonance and 9.6 fb^{-1} recorded 40 MeV below it, with the *BABAR* detector [4] at the PEP-II asymmetric-energy e^+e^- collider. We use samples of GEANT Monte Carlo (MC) simulated events that correspond to about three times the data sample size.

The momenta of charged particles are measured by a tracking system consisting of a five-layer silicon vertex tracker (SVT) and a 40-layer drift chamber (DCH), operating in a 1.5-T solenoidal magnetic field. Charged particles of different masses are distinguished by their energy loss in the tracking devices and by a ring-imaging Cherenkov detector. Electromagnetic showers from electrons and photons are measured in a CsI(Tl) calorimeter. Muons are identified in a set of resistive plate chambers inserted in the iron flux-return yoke of the magnet.

We select events that contain a D^{*+} candidate and an oppositely charged electron or muon with momentum $1.2 < p_\ell < 2.4$ GeV/c. [Unless explicitly stated otherwise, momenta are measured in the $\Upsilon(4S)$ rest frame, which does not coincide with the laboratory frame, due to the boost of the PEP-II beams.] In this momentum range, the electron (muon) efficiency is about 90% (60%) and the hadron misidentification rate is typically 0.2% (2.0%). We select D^{*+} candidates in the momentum range $0.5 < p_{D^*} < 2.5$ GeV/c in the channel $D^{*+} \to D^0\pi_s^+$, with the D^0 decaying to $K^-\pi^+$, $K^-\pi^+\pi^-\pi^+$, or $K^-\pi^+\pi^0$. The charged hadrons of the D^0 candidate are fit to a common vertex and the candidate is rejected if the fit probability is less than 0.1%. We require the invariant mass of the hadrons to be compatible with the D^0 mass within ± 2.5 times the experimental resolution. This corresponds to a range of ± 34 MeV/c^2 for the $D^0 \to K^-\pi^+\pi^0$ decay and ± 17 MeV/c^2 for the other decays. For $D^0 \to K^-\pi^+\pi^0$, we accept only candidates from portions of the Dalitz plot where the square of the decay amplitude, as determined by Ref. [5], is at least 10% of the maximum it attains anywhere in the plot. For the pion from D^{*+} decay, π_s^+, the momentum in the laboratory frame must be less than 450 MeV/c, and the transverse momentum greater than 50 MeV/c. Finally, the lepton, π_s^+, and D^0 are fit to a common vertex with a beam-spot constraint, and the probability for this fit is required to exceed 1%.

In semileptonic decays, the presence of an undetected neutrino complicates the separation of the signal from background. We compute a kinematic variable with considerable power to reject background by determining, for each B-decay candidate, the cosine of the angle between the momentum of the $\overline{B}^0$ and of the $D^{*+}\ell^-$ pair, under the assumption that only a massless neutrino is missing:

$$\cos\theta_{B^0,D^*\ell} = \frac{2E_{\overline{B}^0}E_{D^*\ell} - M^2_{\overline{B}^0} - M^2_{D^*\ell}}{2p_{\overline{B}^0}p_{D^*\ell}}.$$

This quantity constrains the direction of the $\overline{B}^0$ to lie along a cone whose axis is the direction of the $D^{*+}\ell^-$ pair, but with an undetermined azimuthal angle about the cone's axis. The value of w varies with this azimuthal angle; we take the average of the minimum and maximum values as our estimator $\tilde{w}$ for w. This results in a resolution of 0.04 on w. We divide the sample into 10 bins in $\tilde{w}$ from 1.0 to 1.5, with the last bin extending to the kinematic limit of 1.504.

The selected events are divided into six subsamples, corresponding to the two leptons and the three D^0 decay modes. In addition to signal events, each subsample contains backgrounds from six different sources: combinatorics (events from $B\overline{B}$ and continuum in which at least one of the hadrons assigned to the D^{*+} does not originate from D^{*+} decay); continuum ($D^{*+}\ell^-$ combinations from $e^+e^- \to c\bar{c}$); fake leptons (combined with a true D^{*+});

uncorrelated background (ℓ and D^{*+} produced in the decay of two different B mesons); events from $B \to D^{*+}\pi\ell^-\overline{\nu}_\ell$ decays; and correlated background events due to the processes $\overline{B}^0 \to D^{*+}\bar{\nu}\tau^-$, $\tau^- \to \ell^- X$ and $\overline{B}^0 \to D^{*+}X_c$, $X_c \to \ell^- Y$. We estimate correlated background (which amounts to less than 0.5% of the selected candidates) from Monte Carlo simulation based on measured branching fractions [6], while we determine all the others from the data. Except for the combinatorics background, all other background sources exhibit a peak in the $\Delta M = M_{D^{*+}} - M_{D^0}$ distribution, where $M_{D^{*+}}$ and M_{D^0} are the measured D^{*+} and D^0 candidate masses.

We determine the composition of the subsamples in each $\tilde{w}$ bin in two steps. First we estimate the amount of combinatorics, continuum, and fake-lepton background by fitting the ΔM distributions in the range $0.139 < \Delta M < 0.165$ GeV/c^2 simultaneously to three sets of events: data recorded on-resonance, data taken below the $\Upsilon(4S)$ (thus containing only continuum background), and data in which tracks that fail very loose lepton-selection criteria are taken as surrogates for fake leptons. The distributions are fit with the sum of two Gaussian functions with a common mean and different widths to describe $D^{*+} \to D^0\pi_s^+$ decays and empirical functions, based on the simulation, for the combinatorics background. The four parameters of the Gaussian functions are common, while the fraction of peaking events and the parameters describing the combinatorics background differ for the signal, off-peak, and fake-lepton samples.

Since the ΔM resolution depends on whether or not the π_s^+ track is reconstructed only in the SVT or in the SVT and DCH, the fits are performed separately for these two classes of events. We rescale the number of continuum and fake-lepton events in the mass range $0.143 < \Delta M < 0.148$ GeV/c^2, based on the relative on- and off-resonance luminosity and measured hadron misidentification probabilities. In the subsequent analysis we fix the fraction of combinatorics, fake-lepton, and continuum events in each $\tilde{w}$ bin to the values so obtained. Figure 1 shows the ΔM fit results for the on-resonance data.

In a second step, we fit the $\cos\theta_{B^0,D^*\ell}$ distributions in the range $-10 < \cos\theta_{B^0,D^*\ell} < 5$ and determine the signal contribution and the normalization of the uncorrelated and $B \to D^{*+}\pi\ell^-\overline{\nu}_\ell$ backgrounds. Neglecting resolution effects, signal events meet the obvious constraint $|\cos\theta_{B^0,D^*\ell}| < 1$, while $B \to D^{*+}\pi\ell^-\overline{\nu}_\ell$ events extend below -1, and uncorrelated background events are spread over the entire range considered.

We perform the fit separately for each $\tilde{w}$ bin, with the individual shapes for the signal and for each of the six background sources taken from MC simulation, specific for each of the six subsamples. Signal events are generated with the form-factor parametrization of Ref. [7], tuned to the results from CLEO [8]. Radiative decays ($\overline{B}^0 \to D^{*+}\ell^-\overline{\nu}_\ell\gamma$) are modeled by PHOTOS [9] and treated as

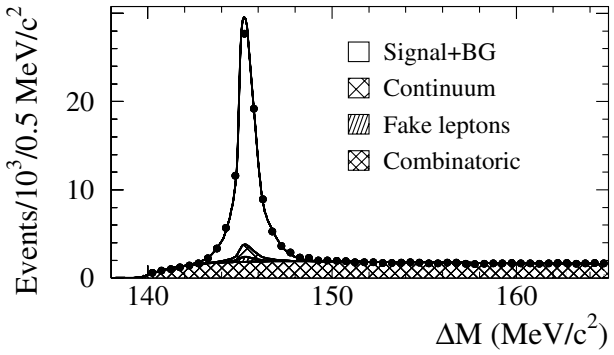

FIG. 1. Yields of on-resonance data (points) and the results of the fit (line) to the ΔM distribution, with contributions from continuum, fake-lepton, and combinatorics-D^{*+} backgrounds summed over all $\tilde{w}$ bins.

signal. $B \to D^{**}\ell\nu$ decays involving orbitally excited charm mesons are generated according to the ISGW2 model [10], and decays with nonresonant charm states are generated following the prescription in Ref. [11]. To reduce the sensitivity to statistical fluctuations we require that the ratio of $B \to D^{*+}\pi\ell^-\overline{\nu}_\ell$ and of uncorrelated background to the signal be the same for all three D^0 decay modes and for the electron and muon samples. Fit results are shown in Fig. 2. In total, there are 70 822 events in the range $|\cos\theta_{B^0,D^*\ell}| < 1.2$. The average fraction of these events that are signal is $(75.9 \pm 0.3)\%$, where the error is only statistical.

To extract $|V_{cb}|$, we compare the signal yields to the expected differential decay rate

$$\frac{d\Gamma}{dw} = \frac{G_F^2}{48\pi^3} M_{D^{*+}}^3 (M_{\overline{B}^0} - M_{D^{*+}})^2 \mathcal{G}(w)\mathcal{F}(w)^2 |V_{cb}|^2,$$

where

$$\mathcal{G}(w) = \sqrt{w^2-1}(w+1)^2\left(1 + 4\frac{w}{w+1}\frac{1-2wr+r^2}{(1-r)^2}\right)$$

is a phase-space factor, $r = M_{D^{*+}}/M_{\overline{B}^0}$. We parametrize the form factor $\mathcal{F}(w)$ with a Taylor expansion:

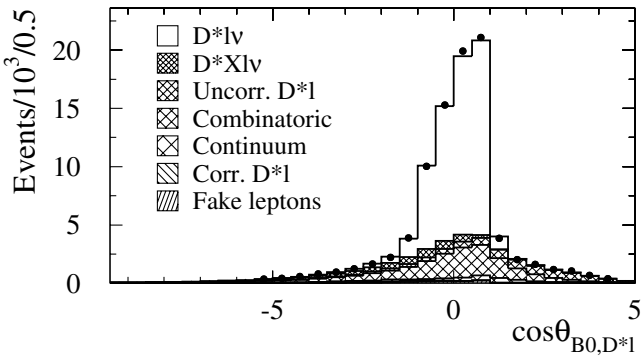

FIG. 2. Yields of on-resonance data (points) and the results of the fit (histograms) to the $\cos\theta_{B^0,D^*\ell}$ distribution, summed over all $\tilde{w}$ bins.

$$\mathcal{F}(w) \approx \mathcal{F}(1)[1 - \rho^2_{\mathcal{F}}(w-1) + c(w-1)^2],$$

where we neglect terms of power greater than two in $(w-1)$. We fit the data to determine $\mathcal{F}(1)|V_{cb}|$, $\rho_{\mathcal{F}}$ and c.

Dispersion relations inspired by QCD can be used to constrain the shape of the form factor and reduce the number of parameters to be determined [7,12]. Therefore we consider also the parametrization proposed in Ref. [7], which relates $\mathcal{F}(w)$ to the axial-vector form factor $\mathcal{A}_1(w)$ according to the following expression

$$\mathcal{F}(w)^2\mathcal{G}(w) = \mathcal{A}_1(w)^2\sqrt{w^2-1}(w+1)^2 \times\left\{2\left[\frac{1-2wr+r^2}{(1-r)^2}\right]\left[1+R_1(w)^2\frac{w-1}{w+1}\right] + \left[1+(1-R_2(w))\frac{w-1}{1-r}\right]^2\right\},$$

where $R_1(w) \approx R_1(1) - 0.12(w-1) + 0.05(w-1)^2$, $R_2(w) \approx R_2(1) + 0.11(w-1) - 0.06(w-1)^2$, and we use the values $R_1(1) = 1.18 \pm 0.32$ and $R_2(1) = 0.71 \pm 0.21$ measured by CLEO [8]. Using dispersion relations we express the ratio $\mathcal{A}_1(w)/\mathcal{A}_1(1)$ as a function of a single unknown parameter $\rho^2_{\mathcal{A}_1}$:

$$\frac{\mathcal{A}_1(w)}{\mathcal{A}_1(1)} \approx 1 - 8\rho^2_{\mathcal{A}_1}z + (53\rho^2_{\mathcal{A}_1} - 15)z^2 - (231\rho^2_{\mathcal{A}_1} - 91)z^3,$$

where $z = (\sqrt{w+1} - \sqrt{2})/(\sqrt{w+1} + \sqrt{2})$. It must be noted that, for $w \to 1$, $\mathcal{A}_1(w) \to \mathcal{F}(w)$, so we expect $\mathcal{A}_1(1) \approx \mathcal{F}(1)$.

We perform a least-squares fit of the sum of the observed signal plus background yields to the expected yield in the ten bins in $\tilde{w}$. We define for each of the six data subsamples

$$\chi^2 = \sum_{i=1}^{10} \frac{\left(N^i_{\rm data} - N^i_{\rm bk} - \sum_{j=1}^{N^i_{\rm MC}} W^i_j\right)^2}{N^i_{\rm data} + \sigma^{i2}_{\rm bk} + \sum_{j=1}^{N^i_{\rm MC}} W^{i2}_j},$$

where $N^i_{\rm data}$ is the number of observed events in the ith bin; $N^i_{\rm bk}$ and $\sigma^i_{\rm bk}$ are the number of estimated background events and its error. The backgrounds are fixed to the estimated rates. The expected signal yield is calculated at each step of the minimization from the reweighted sum of N^i_{MC} simulated events. Each weight is the product of four weights, $W^i_j = W^{\mathcal{L}}W^{\epsilon,i}_j W^S W^{ff,i}_j$. The factors $W^{\mathcal{L}}$, $W^{\epsilon,i}_j$ do not vary during the minimization, while the terms W^S, $W^{ff,i}_j$ depend on parameters which are determined by the fit, and vary at each step of the minimization.

The first factor $W^{\mathcal{L}}$ accounts for relative normalization of the data and MC samples, and is common to all subsamples. $W^{\mathcal{L}}$ depends on the total number of $B\overline{B}$ events, $N_{B\overline{B}} = (85.9 \pm 0.9) \times 10^6$, on the fraction of $B^0\overline{B}^0$ events, $f_{00} = 0.489 \pm 0.012$ [6], on the branching fraction $\mathcal{B}(D^{*+} \to D^0\pi^+) = 0.677 \pm 0.005$ [6], and on the B^0 lifetime $\tau_{B^o} = 1.536 \pm 0.014$ ps [6]. $W^{\epsilon,i}_j$ accounts for differences in reconstruction and particle-identification efficiencies predicted by the Monte Carlo simulation and measured with data, as a function of particle momentum. Only the π^+_s tracking efficiency varies significantly with $\tilde{w}$.

The weight W^S accounts for potential small differences in efficiencies for the six data subsamples and allows for adjustments of the D^0 branching fractions, properly dealing with the correlated systematic uncertainties. It is the product of several scale factors that are floating parameters in the fit, each constrained to an expected value with a corresponding experimental error. For instance, to account for the uncertainty in the multiplicity-dependent tracking efficiency, we introduce a factor $W^S_{trk} = 1 + N_{trk}\delta_{trk}$, where N_{trk} is the number of charged tracks in the $D^{*+}\ell^-$ candidates in each sample. The parameter δ_{trk} represents the possible residual difference between the actual single-track reconstruction efficiency and the one predicted by the simulation, already corrected for the known discrepancies between data and Monte Carlo predictions using the weight $W^{\epsilon,i}_j$. We allow δ_{trk} to vary in the fit, constraining its value to zero within the experimental uncertainty in the single-track reconstruction efficiency, $\pm 0.8\%$. Similarly, correction factors are introduced to adjust lepton, kaon, and π^0 efficiencies, and D^0 branching fractions, taking into account correlations.

The fourth factor, $W^{ff,i}_j$, adjusts the fitted decay distribution relative to the one used in the generation of the MC events. This term depends on $|V_{cb}|$ and on the shape parameters. It is a function of w and is determined for each simulated event at each step of the fit.

Figure 3 (top) compares the observed signal and background yields, summed over all six subsamples, with the result of the fit. Figure 3 (bottom) illustrates the extrapolation to $w = 1$ for the two form-factor parametrizations. The numerical values obtained for the two different form-factor parametrizations are listed in Table I. For both fits, the χ^2 per degree of freedom is satisfactory, and the scale factors introduced to allow adjustments of the efficiencies and branching fractions deviate from their default values by less than one standard deviation.

In Table II we present a summary of the statistical and systematic uncertainties. From the fit to the $\tilde{w}$ distribution we obtain errors that combine the statistical error with systematic errors introduced by the uncertainties in scale factors. We separate the various contributions in the following way: first, we extract the statistical errors by fixing all scale factors to their fitted values. The systematic errors due to the uncertainties in a given scale factor are extracted from a separate fit in which this scale factor is fixed. We take the square root of reduction in the square of the fit errors as a measure of the contribution of the particular scale factor to the overall error in the fit parameters.

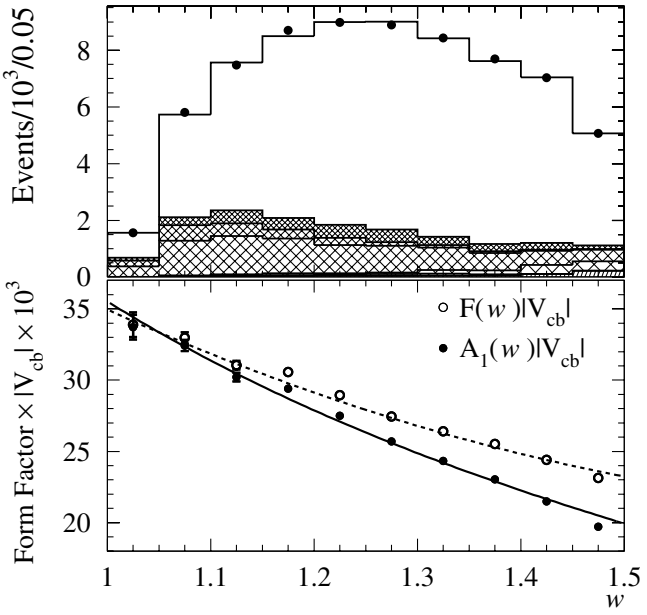

FIG. 3. Results of the fit as a function of $\tilde{w}$ compared to data. Top: the observed $\tilde{w}$ distribution (points) compared to the fit result; signal and background contributions are indicated using the same shading as in Fig. 2. Bottom: the form-factor parametrizations with fitted parameters compared to the background- and efficiency-corrected data. The solid (dotted) line corresponds to the $\mathcal{A}_1(w)$ ($\mathcal{F}(w)$) parametrization, and is to be compared to the filled (open) data points.

We then assess the individual contributions to the systematic error due to other input quantities by varying their values by their estimated uncertainties and adding in quadrature the resulting changes to the fit parameters. The uncertainties in the lifetime τ_{B^0}, the $\Upsilon(4S)$ and D^{*+} branching fractions, and overall normalization are independent of w and thus do not affect the shape of the form factor. The uncertainty introduced by the vertex reconstruction is common to all samples and independent of w. It is determined by comparing the event samples with and without cuts on the vertex probability. The error induced by the cut on the decay amplitude for the $K^-\pi^+\pi^0$ decay is determined by varying that cut.

A major source of uncertainty is the reconstruction efficiency for the low-momentum pion from the D^{*+} decay, since it is highly correlated with the D^{*+} momentum and thereby with w. We determine the tracking efficiency

TABLE I. Results of the fits to $d\Gamma/d\tilde{w}$ for the two parametrizations of the form factor. The errors stated include statistical error of the data and MC as well as uncertainties due to tracking, particle-identification, and D^0 branching fractions that are directly assessed in the fit procedure.

	$\mathcal{A}_1(1)\lvert V_{cb}\rvert \times 10^3$	ρ^2	c	χ^2/ndf
$\mathcal{F}$	35.0 ± 0.9	0.95 ± 0.09	0.54 ± 0.17	67/57
$\mathcal{A}_1$	35.5 ± 0.8	1.29 ± 0.03		69/58

TABLE II. Summary of uncertainties.

Source of uncertainty	$\delta(\mathcal{A}_1(1)\lvert V_{cb}\rvert)$ (%)	$\delta\rho^2_{\mathcal{A}_1}$	$\delta\mathcal{B}$ (%)
Data and MC statistics	0.7	0.03	1.4
$\mathcal{B}(D^0 \to K^-\pi^+)$	1.1		2.2
$\mathcal{B}(D^0 \to K^-\pi^+\pi^-\pi^+)$	0.4		0.8
$\mathcal{B}(D^0 \to K^-\pi^+\pi^0)$	0.5		1.0
Particles identification	1.1		2.2
Tracking and π^0 reconstruction	1.3		2.6
Partial sum	2.2	0.03	4.5
B^0 lifetime	0.5		
Number of $B\overline{B}$	0.6		1.2
$\mathcal{B}(D^{*+} \to D^0\pi^+)$	0.4		0.7
$\mathcal{B}(\Upsilon(4S) \to B^0\overline{B}^0)$	1.2		2.5
$D^{*+}\ell^-$ vertex efficiency	0.5		1.0
π_s efficiency	1.1	0.01	1.9
$D^*\pi\ell\nu$ sample composition	1.8	0.06	2.0
B momentum	0.3		0.7
Radiative corrections	0.2	0.01	0.4
$\cos\theta_{B^0,D^*\ell}$ and $\tilde{w}$ fit method	0.8	0.02	1.6
$R_1(1)$ and $R_2(1)$	$^{+2.9}_{-2.6}$	0.26	$^{+3.9}_{-3.3}$
Total error	$^{+4.6}_{-4.4}$	0.27	$^{+7.4}_{-7.1}$

for high-momentum tracks comparing the independent information from SVT and DCH. We compute the efficiency for low-momentum tracks reconstructed in the SVT alone from the angular distribution of the π_s^+ in the D^{*+} rest frame. We use a large set of $D^{*+} \to D^0\pi_s^+$, $D^0 \to K^-\pi^+$ decays selected from generic hadronic events. For fixed values of the D^{*+} momentum, we compare the observed angular distribution to the one expected for the decay of a vector meson to two pseudoscalar mesons. We define the relative efficiency as the ratio of the observed to the expected distribution and parameterize its dependence on the laboratory momentum of the π_s^+. The study is performed in several bins of the polar angle of the detector. We perform the measurement in the data and in the simulation, and we find that the functions parameterizing the efficiency are consistent within the statistical errors. To assess the systematic uncertainty on $|V_{cb}|$, we vary the parameters of the efficiency function by their uncertainty, including correlations. We add in quadrature the uncertainty in the absolute scale, as determined using high-momentum tracks reconstructed in both the SVT and the DCH. We obtain a systematic error of $\pm 1.1\%$ on $|V_{cb}|$.

The largest error in the background subtraction is due to the uncertainty in the composition and form factors of the $D^{*+}\pi\ell^-\bar{\nu}_\ell$ decays. We consider twelve different $D^{*+}\pi$ states, narrow and wide, as well as nonresonant $D^{*+}\pi$. To assess the impact of these decays on the fit we repeat the analysis assuming that only one mode at a time populates the whole sample, and then take as the systematic error half the difference between the maximum and minimum fitted parameters.

We assess the effect of the uncertainty in the average $\overline{B}^0$ momentum, as determined from a sample of fully recon-

structed hadronic B decays on the fit results. We take into account an uncertainty of $\pm 30\%$ in the emission rate of the radiative photons predicted by PHOTOS [9].

We also assess the impact of changes in the bin size on the fits to the $\cos\theta_{B^0,D^*\ell}$ and $\tilde{w}$ distributions.

There are several uncertainties related to the form factors and their parametrization. The form-factor ratios R_1 and R_2 affect the lepton momentum spectrum and thus the differential decay rate as a function of w, as well as the fraction of events satisfying the lepton momentum requirements. We assess these effects by varying R_1 and R_2 within the measurement errors [8], taking into account their correlation. As a consistency check, we compare the measured momentum spectra of the D^{*+} and leptons with the spectra expected from the fit results. We find very good agreement for the D^{*+}, but the lepton spectrum favors a larger value for R_1, though one consistent with the available measurement.

If we fit separately e and μ samples, we find exactly the same value for $\rho^2_{\mathcal{A}_1}$. The values of $\mathcal{A}_1|V_{cb}|$, $(35.8 \pm 0.5) \times 10^{-3}$ and $(35.0 \pm 0.5) \times 10^{-3}$, respectively, differ by 1.2 standard deviation.

The value of c, given in Table I, shows that the data disfavor a purely linear dependence of $\mathcal{F}$ on w, by almost three standard deviations. The fits for the two different parametrizations of the w dependence of the form factors are consistent at $w = 1$. We choose $\mathcal{A}_1(1)|V_{cb}| = (35.5 \pm 0.3 \pm 1.6) \times 10^{-3}$, and $\rho^2_{\mathcal{A}_1} = 1.29 \pm 0.03 \pm 0.27$, where the errors listed refer to the statistical, and the systematic uncertainties. The correlation between $\mathcal{A}_1(1)|V_{cb}|$ and $\rho^2_{\mathcal{A}_1}$ is 0.56, taking into account statistical and systematic errors. A recent lattice calculation [3] (including a QED correction of 0.7%) gives $\mathcal{A}_1(1) = \mathcal{F}(1) = 0.919^{+0.030}_{-0.035}$, with which we obtain

$$|V_{cb}| = (38.7 \pm 0.3 \pm 1.7^{+1.5}_{-1.3}) \times 10^{-3},$$

where the first error is statistical, the second is systematic, and the third reflects the uncertainty in $\mathcal{A}_1(1)$. Integrating over the fitted $\tilde{w}$ distribution these parameters result in the branching fraction $\mathcal{B}(\overline{B}^0 \to D^{*+}\ell^-\bar{\nu}_\ell) = (4.90 \pm 0.07^{+0.36}_{-0.35})\%$, where the errors are the statistical and systematic uncertainties.

In summary, we have measured the CKM parameter $|V_{cb}|$ and the exclusive branching fraction for $\overline{B}^0 \to D^{*+}\ell^-\bar{\nu}_\ell$ with high precision. The result for $|V_{cb}|$ is consistent with another *BABAR* measurement based on lepton and hadron spectra from inclusive semileptonic B-meson decays [13], $|V_{cb}| = (41.4 \pm 0.4(\text{stat.}) \pm 0.4(\text{exp.}) \pm 0.6(\text{theory})) \times 10^{-3}$. The results for $|V_{cb}|$ and the branching fraction are also consistent with earlier measurements [14] based on the technique employed here, except for those from the CLEO experiment [15].

We are grateful for the excellent luminosity and machine conditions provided by our PEP-II colleagues, and for the substantial dedicated effort from the computing organizations that support *BABAR*. The collaborating institutions wish to thank SLAC for its support and kind hospitality. This work is supported by DOE and NSF (U.S.), NSERC (Canada), IHEP (China), CEA and CNRS-IN2P3 (France), BMBF and DFG (Germany), INFN (Italy), FOM (The Netherlands), NFR (Norway), MIST (Russia), and PPARC (United Kingdom). Individuals have received support from the A. P. Sloan Foundation, Research Corporation, and Alexander von Humboldt Foundation. His colleagues would like to acknowledge the enthusiasm and expertise that Paolo Poropat brought to our Collaboration.

[1] Charge conjugate decay modes are implicitly included, $\ell = e, \mu$.
[2] N. Isgur and M. B. Wise, Phys. Lett. B **232**, 113 (1989); **237**, 527 (1990).
[3] S. Hashimoto *et al.*, Phys. Rev. D **66**, 014503 (2002).
[4] *BABAR* Collaboration, B. Aubert *et al.*, Nucl. Instrum. Methods Phys. Res., Sect. A **479**, 1 (2002).
[5] E687 Collaboration, P. L. Fabretti *et al.*, Phys. Lett. B **331**, 217 (1994).
[6] Particle Data Group, S. Eidelman *et al.*, Phys. Lett. B **592**, 1 (2004).
[7] I. Caprini, L. Lellouch, and M. Neubert, Nucl. Phys. **B530**, 153 (1998).
[8] CLEO Collaboration, J. E. Duboscq *et al.*, Phys. Rev. Lett. **76**, 3898 (1996).
[9] E. Barberio and Z. Was, Comput. Phys. Commun. **79**, 291 (1994).
[10] D. Scora and N. Isgur, Phys. Rev. D **52**, 2783 (1995).
[11] J. L. Goity and W. Roberts, Phys. Rev. D **51**, 3459 (1995).
[12] C. G. Boyd, B. Grinstein, and R. F. Lebed, Phys. Rev. D **56**, 6895 (1997).
[13] *BABAR* Collaboration, B. Aubert *et al.*, Phys. Rev. Lett. **93**, 011803 (2004).
[14] ARGUS Collaboration, H. Albrecht *et al.*, Phys. Lett. B **324**, 249 (1994); ALEPH Collaboration, D. Buskulic *et al.*, Phys. Lett. B **395**, 373 (1997); DELPHI Collaboration, P. Abreu *et al.*, Z. Phys. C **71**, 539 (1996); Phys. Lett. B **510**, 55 (2001); OPAL Collaboration, G. Abbiendi *et al.*, Phys. Lett. B **482**, 15 (2000); BELLE Collaboration, K. Abe *et al.*, Phys. Lett. B **526**, 247 (2002).
[15] CLEO Collaboration, R. A. Briere *et al.*, Phys. Rev. Lett. **89**, 081803 (2002); CLEO Collaboration, N. E. Adam *et al.*, Phys. Rev. D **67**, 032001 (2003).